

# 1 Temperature variability of the Iberian Range since 1602 2 inferred from tree-ring records

3  
4  
5 **E. Tejedor<sup>1,2,3</sup>, M.A. Saz<sup>1,2</sup>, J.M. Cuadrat<sup>1,2</sup>, J. Esper<sup>3</sup>, M. de Luis<sup>1,2</sup>**

6 [1]{University of Zaragoza, 50009 Zaragoza, Spain}

7 [2]{Environmental Sciences Institute of the University of Zaragoza}

8 [3]{Department of Geography, Johannes Gutenberg University, 55099 Mainz, Germany}

9 Correspondence to: E. Tejedor (etejedor@unizar.com)

## 10 11 **Abstract**

12 Tree-rings are an important proxy to understand the natural drivers of climate variability in  
13 the Mediterranean basin and hence to improve future climate scenarios in a vulnerable region.  
14 Here, we compile 316 tree-ring width series from 11 conifer sites in the western Iberian  
15 Range. We apply a new standardization method based on the trunk basal area instead of the  
16 tree cambial age to develop a regional chronology which preserves high to low frequency  
17 variability. A new reconstruction for the 1602-2012 period correlates at -0.78 with  
18 observational September temperatures with a cumulative mean of the 21 previous months  
19 over the 1945-2012 calibration period. The new IR2T<sub>max</sub> reconstruction is spatially  
20 representative for the Iberian Peninsula and captures the full range of past Iberian Range  
21 temperature variability. Reconstructed long-term temperature variations match reasonably  
22 well with solar irradiance changes since warm and cold phases correspond with high and low  
23 solar activity, respectively. In addition, some annual temperatures downturns coincide with  
24 volcanic eruptions with a three year lag.

## 25 26 **1 Introduction**

27 The IPCC report (IPCC, 2013) highlighted a likely increase of average global temperatures in  
28 upcoming decades, and pointed particularly to the Mediterranean basin, and therefore in the

1 Iberian Peninsula (IP), as a region of substantial modelled temperature changes. The  
2 Mediterranean area is located in the transitional zone between tropical and extra-tropical  
3 climate systems, characterized by a complex topography and high climatic variability (Hertig  
4 and Jacobeit 2008). Taking into account these features, even relatively minor modifications of  
5 the general circulation, i.e. a shift in the location of sub-tropical high pressure cells, can lead  
6 to substantial changes in Mediterranean climate (Giorgi and Lionello 2008), making the study  
7 area a potentially vulnerable region to anthropogenic climatic changes by anthropogenic  
8 forces, i.e. increasing concentrations of greenhouse gases (Lionello et al., 2006a; Ulbrich et  
9 al., 2006)

10 Major recent efforts have been made in understanding trends in temperatures throughout the  
11 IP over the instrumental period (Kenaway et al., 2012; Pena-Angulo et al., 2015; Gonzalez-  
12 Hidalgo et al., 2015) and future climate change scenarios (Sánchez et al., 2004; López-  
13 Moreno et al., 2014). However, the fact that most of the observational records do not begin  
14 until the 1950s (Gonzalez-Hidalgo et al., 2011) is limiting the possibility of investigating the  
15 inter-annual to multi-centennial long-term temperature variability. Therefore, it is crucial to  
16 explore climate proxy data and develop long-term reconstructions of regional temperature  
17 variability to evaluate spatial patterns of climatic change and the role of natural and  
18 anthropogenic forcings on climate variations (Büntgen et al., 2005). In the IP, much progress  
19 has been made to reconstruct past centuries climate variability, including analysis of  
20 documentary evidences for temperature (i.e. Camuffo et al., 2010) and droughts  
21 reconstruction (i.e. Barriendos et al. 1997; Cuadrat and Vicente, 2007; Domínguez-Castro et  
22 al., 2010). Additionally, progress has been made to further understanding of long-term climate  
23 variability of the IP through dendroclimatological studies focussing on drought (Esper et al.,  
24 2014; Tejedor et al., 2015) and temperature (Büntgen et al., 2008; Dorado-Liñán et al., 2012,  
25 2014; Esper et al. 2015a). Nevertheless, a high-resolution temperature reconstruction for  
26 central Spain is still missing.

27 Several studies have been made to develop a temperature reconstruction for the Iberian Range  
28 (IR) using *Pinus uncinata* tree-ring data (Creus and Puigdefabreas, 1982; Ruiz, 1989). The  
29 results, in fact, showed a pronounced inter-annual to century scale chronology variability.  
30 However, their main result was a complex growth response function due to a mixed climate  
31 signal instead of a temperature reconstruction. Furthermore, Saz (2003) developed a 500-year  
32 temperature reconstruction for the Ebro Depression (North of Spain), but this chronology is

1 based on a reduced number of cores and a standardized methodology that did not retain the  
2 medium and low frequency variance.

3 Here we present the first tree-ring dataset combining samples from three different sources  
4 from the eastern IR extending back from the Little Ice Age (1465) to present (2012). The aim  
5 of this study is to develop a temperature reconstruction representing the IR, and thereby fill  
6 the gap between records located in the northern and southern IP. A new methodology, based  
7 on basal area instead of the cambial-age, was applied to preserve high-to-low frequency  
8 variance in the resulting chronologies. Furthermore, the relationship between the tree-ring and  
9 climate data is reanalysed by adding memory to the climate parameters, since memory effects  
10 on tree-ring data are much less acknowledged (Anchukaitis et al., 2012). This analysis is  
11 challenging because of the mix of tree species and their unidentified responses to climate. The  
12 resulting reconstruction of September maximum temperatures over the past four centuries is  
13 compared with latest findings from the Pyrenees and Cazorla, and the relationship with solar  
14 and volcanic forcings at inter-annual to multi-decadal timescales.

15

## 16 **2 Material and methods**

### 17 **2.1 Site description**

18 We compiled a tree ring network from 11 different sites in the western IR (Table 1) in the  
19 province of Soria. Urbión is the most extensive forest of the IP including 120,000 ha between  
20 the Burgos and Soria provinces. It has a long forest management tradition. Therefore, all sites  
21 are situated at high elevation locations where forests are least exploited and maximum tree  
22 age is reached (Fig.1). The altitude of the sampling sites ranges from 1,500 to 1,900 meters  
23 above sea level (masl) with a mean of 1,758 masl. These forests belong to the Continental  
24 Bioclimatic Belt (Gujarro, 2013) characterized by moderate mean temperatures (9.5°C,  
25 Fig.2B) and a large seasonal range including more than 90 frost days and summer heat  
26 exceeding 30°C . Mean annual precipitation for the period 1944-2014 is 927 mm (CRU TS.3  
27 v.23 dataset by Harris et al., 2014) and reaches its maximum during December (Fig. 2AC).

28 Although scotts pine (*Pinus sylvestris*) is the dominant tree species of the region, other  
29 pinaceae are found such as *Pinus pinaster*, *Pinus nigra* or *Pinus uncinata*. Especially  
30 remarkable is occurrence of *Pinus uncinata* growing above 1,900 masl and reaching its

1 European southern distribution limits in the IR. The lithology of the study area consists of  
2 sandstones, conglomerates and lutites.

## 3 **2.2 Tree ring chronology development**

4 The new dataset is composed by 316 tree-ring width (TRW) series of *Pinus uncinata* (56) and  
5 *Pinus sylvestris* (260) located in the western IR (Tab. 1, Fig. 1). The most recent samples  
6 were collected during the field campaign in 2013 including old dominant and co-dominant  
7 trees with healthy trunks and no sign of human interference. We extracted two core samples  
8 from each tree at breast height (1.3 m) when possible, otherwise, we try to avoid compression  
9 wood due to steep slopes, compiling a set of 96 new samples from two sites, i.e. the outermost  
10 ring is 2012. Core samples were air-dried and glued onto wooden holders and subsequently  
11 sanded to ease growth ring identification (Stokes and Smiley 1968). The samples were then  
12 scanned and synchronized using CoRecorder software (Larsson 2012) (Cybis  
13 Dendrochronology 2014) to identify the position and exact dating of each ring. The tree-ring  
14 width was measured, at 0.01 mm precision, using LINTAB table (Rinn 2005). Prior to  
15 detrending, COFECHA (Holmes 1983) was used to assess the cross-dating of all  
16 measurement series.

17 An additional set of 95 samples from three sites was provided by the project CLI96-1862  
18 (Creus et al. 1992, Saz 2003) i.e., the outermost rings range from 1992 to 1993. Finally, a set  
19 of 125 samples from five sites was downloaded from the International Tree Ring Data Bank  
20 (ITRDB, <http://www.ncdc.noaa.gov/data-access/paleoclimatology-data/datasets/tree-ring>).  
21 These data were developed in the 1980s by K. Richter and collaborators, i.e. the outermost  
22 rings range from 1977 to 1985.

23 In order to attempt a climate reconstruction for the western IR from this tree-ring network, we  
24 perform an exploratory analysis of the 11 tree-ring chronologies by creating a correlation  
25 matrix of the raw chronologies for each site for the common period (1842-1977) and for the  
26 full period (1465-2012).

### 27 **2.2.1 Standardization methods**

28 The key concept in dendroclimatology is referred to as the standardization process (Fritts,  
29 1976; Cook et al., 1990) where the aim is to preserve as much of the climate-related  
30 information as possible while removing the non-climatic information from the raw TRW



1 measurements. However, with most of the standardization methods a varying proportion of  
2 the low-frequency climatic information is also lost in the process (Grudd, 2008). When the  
3 aim is to use tree-ring chronologies as a proxy for climatic reconstructions, an adequate  
4 standardization is critical and the best method should preserve high to low frequency  
5 variations (Büntgen et al., 2004). It is common practice to calculate a mean value function as  
6 the best estimate of the trees' signal at a site (Frank et al., 2006).

7 We here applied four standardization methods to the 316 TRW measurement series to develop  
8 a single tree-ring index chronology. (i) To emphasize inter-decadal and higher frequency  
9 variations, each ring width series was fitted with a cubic spline with a 50% frequency  
10 response cut off at 67% of the series length (Cook et al., 1990). A bi-weight robust mean was  
11 calculated to assemble the ArstanSTD regional chronology. (ii) A residual chronology  
12 (ArstanRES) is produced after removing first-order autoregression to emphasize high-  
13 frequency variability. (iii) To preserve common inter-decadal and lower frequency variations,  
14 Regional Curve Standardization (RCS) was applied (Mitchell, 1967; Briffa et al., 1992, 1996;  
15 Esper et al., 2003). RCS is an age-dependent composite method and involves dividing the size  
16 of each tree-ring by the value expected from its cambial age. To assemble the chronology, all  
17 the series are aligned by cambial age. A single growth function (regional curve, RC)  
18 smoothed using a spline function of 10% of the series length is fit to the mean of all age-  
19 aligned series. A biweight robust mean was applied to develop the RCS chronology (RCS).  
20 (iv) To preserve high to low frequency variance, we additionally applied a novel  
21 standardization method based on the principles of RCS. However, instead of using the  
22 cambial age of the trees as the independent variable, we used their sizes, calculated as the  
23 square of the basal area of the tree in the year prior to ring formation. Then, a Poisson  
24 regression model was used to fit the individual tree-ring widths. Standardized indices were  
25 calculated as the ratio between the observed and predicted values, and a biweight robust mean  
26 was used to develop the Basal Area Poisson chronology (BasPois).

27 To evaluate uncertainty of the mean chronologies running interseries correlations ( $R_{bar}$ ) and  
28 the express population signal (EPS) were calculated (Wigley et al., 1984).  $R_{bar}$  is a measure  
29 of the strength of the common growth 'signal' within the chronology (Wigley et al. 1984;  
30 Briffa and Jones, 1990), here calculated in a 50-year window sliding along the chronology.  
31 EPS is an estimate of the chronology's ability to represent the signal strength of a chronology  
32 on a theoretical infinite population (Wigley et al., 1984).

### 1 **2.3 Climatic data, calibration and climate reconstruction**

2 Monthly temperature (mean, maximum, and minimum) and precipitation values from the  
3 gridded CRU TS v.3.22 dataset (0.5° resolution) dataset for the period 1945-2012 were used  
4 (Harris et al. 2014). The three grid points closest to the tree-ring network were averaged to  
5 develop a regional time series (Fig. 1). In addition, we calculate a cumulative monthly mean  
6 for each of the four parameters (max., min., mean temperature, and monthly precipitation).  
7 The cumulative mean is calculated by adding the months gradually. First the previous month  
8 is added, and then further months are included up to 36 previous months. For the calculations  
9 we take into account the current and the previous year.

10 For calibration, we correlated the four chronologies (ArstanSTD, ArstanRES, RCS, and  
11 BasPois) with monthly climate data and the cumulative monthly mean derived. To assess the  
12 stability of the correlation, we calculated a 30-year moving correlation shifted along 1945-  
13 2012 with the cumulative monthly mean from the current and the previous year. In addition,  
14 the maximum and minimum differences between the moving correlations were calculated. As  
15 a result, the climatic variable chosen for the reconstruction is supported by having the highest  
16 moving correlation with the least difference between the maximum and the minimum over the  
17 moving correlation period.

18 A split calibration/verification approach was perform over the periods 1945-1978 and 1979-  
19 2012 to evaluate the accuracy of the transfer model considering the following metrics;  
20 Pearson's correlation ( $r$ ), coefficient of determination ( $r^2$ ), reduction of error (RE), mean  
21 square error (MSE), and sign test (Cook et al., 1994).  $R$  is a measure of the linear correlation  
22 between the chronology and climatic variable.  $R^2$  indicates how well the data fit a statistical  
23 model. An  $r^2$  of 1 indicates that the regression line perfectly fits the data; an  $r^2$  of 0 indicates  
24 that there is not fit at all. RE is a measure of shared variance between actual and estimated  
25 series and provides sensitive measure of the reliability of a reconstruction (Cook et al., 1994;  
26 Akkemik et al., 2005; Büntgen et al., 2008); it ranges from +1 indicating perfect agreement, to  
27 minus infinity. MSE estimates the difference between the modelled and measured while sign  
28 test compares the number of agreeing and disagreeing interval trends, from year-to-year,  
29 between the observed and reconstructed series (Fritts et al., 1990; Cufar et al., 2008).  
30 Additionally, a Superposed Epoch Analysis (SEA; Panofsky and Brier, 1958) was performed  
31 using dplr (Bunn, 2008) to assess post-volcanic cooling signals in our reconstruction. The  
32 approach has been used in studies of volcanic effect on climate (Fischer et al., 2007; D'Arrigo

1 et al., 2009; Esper et al. 2013a, 2013b). The major volcanic events chosen for the analysis  
2 were those identified by Crowley (2000).

3 To transfer the TRW chronology into a temperature reconstruction a linear regression model  
4 was used. The magnitude and the spatial extent of the climate signal are evaluated considering  
5 the CRU TS v. 3.22 gridded dataset for Europe.

6

### 7 **3 Results**

8 The correlation matrix (Fig. 3) shows not only the high inter-correlation between sampling  
9 sites and tree species but also the high correlation between each chronology and the regional  
10 chronology. The highest correlation is found between *Pinus uncinata* (VIN and CAV) located  
11 at the highest altitude. On the other hand, the weakest correlation is found between one of the  
12 lowest sites (s006) and the highest (VIN). The mean correlation among all sampling sites is  $r$   
13 = 0.51 over the common period (1842-1977) is 0.51, and  $r = 0.46$  over the full period of  
14 overlap, revealing a regionally common, external forcing controlling tree growth and  
15 justifying the development of a single chronology integrating the data from this IP tree-ring  
16 network.

17 The model (regional curve) of the RCS standardization method and the model of the BasPois  
18 method are presented in Fig.4. BasPois model (Fig.4a) indicates a growth of 130 mm when  
19 the size of the basal area is near 0 and a growth of 8mm when it reaches the maximum basal  
20 area. RCS model (Fig.4b) presents values of 250 mm of growth when the cambial age is 0  
21 with a gradual decline of the growth until the cambial of 450. Cambial age from 500 to 550  
22 has a slight increase in growth most likely derived by low replication regarding trees with this  
23 age.

24 Calibration of the four differently detrended mean chronologies reveals a highly negative  
25 correlation with maximum temperatures (Fig. 5). The ArstanRES chronology shows moderate  
26 correlations with previous-year September ( $r = -0.25$ ), and the ArstanSTD chronology  
27 correlates at  $r = -0.38$  with June and September temperature of the previous year. Considering  
28 the RCS chronology, the previous-year September signal increases to  $r = -0.49$  with a  
29 cumulative monthly mean of 21 months. Finally, the best correlations is revealed for the  
30 BasPois chronology reaching  $r = -0.78$  with maximum September temperature of the previous  
31 year with a cumulative mean of 21 months, which is, in fact a two year cumulative monthly

1 mean. Even though the signals show the same seasonal patterns among the chronologies, the  
2 BasPois record always shows the highest correlations. Accordingly, we used the BasPois  
3 chronology for the calibration and reconstruction process.

4 The final BasPois network chronology (Fig.6) is based on 316 TRW series of *Pinus uncinata*  
5 and *Pinus sylvestris* spanning the 1465-2012 period. Since this chronology is derived from  
6 only living trees, mean chronology age increases from 47 years in 1966 to 528 in 1465. The  
7 mean sensitivity is 0.21, and first-order autocorrelation is 0.83. The inter-series correlation  
8 ( $R_{bar}$ ) reaches 0.26, and the first principal component explains about 35% of the variance.  
9 The network chronology's signal to noise ratio is 48.52, and EPS exceeds 0.85 after 1602,  
10 constraining the reconstruction period to 410 years until 2012.

11 The selection of the best climate parameter to develop the reconstruction is presented in the  
12 Figure 7 where correlations between -0.54 and -0.86 representing only the most significant  
13 values are shown. Four parameters reveal the highest correlations over the full calibration  
14 period: October of the current year with a cumulative monthly mean of 22 months; September  
15 of the previous year with a cumulative monthly mean of 20-months; September of the  
16 previous year with a cumulative monthly mean of 21months; and October of the previous year  
17 with a cumulative monthly mean of 21 months. The stability of the correlation and therefore  
18 the consistency of the signal are tested considering the minimum difference between the  
19 maximum and minimum correlation (Fig. 7b) over the full running correlation period. The  
20 smallest difference (0.24) is reached for September of the previous year with a cumulative  
21 monthly mean of 21months. Therefore, this parameter is chosen for the climate  
22 reconstruction. According to the 30-year moving correlations, maximum values are reached  
23 from 1973-2003 ( $r = -0.80$ ), whereas the lowest 30-year correlation ( $r = -0.60$ ) is reached from  
24 1956-1986. In addition, the relationship between September of the previous year with a  
25 cumulative monthly mean of 21months is spatially consistent throughout the Iberian  
26 Peninsula, reaching into southern France and northern Africa (Fig.11).

27

28 The transfer model is validated by the high correlation ( $r = -0.78$ ) and significant coefficient  
29 of determination ( $r^2 = 0.61$ ) over the full period 1945-2012. Through the split  
30 calibration/verification process, considering 1945-1978 and 1979-2012, the temporal  
31 robustness was tested revealing highly significant correlations for both periods ( $r^2=0.41$  and  
32  $r^2=0.55$  respectively) and verifying the final reconstruction (Table 2 and Fig. 8). To develop

1 the final reconstruction spanning 1602-2012, we used a lineal regression model over the full  
2 period 1945-2012 with maximum temperature of September of the previous year with a  
3 cumulative monthly mean of 21months (Eq.1), denominated IR2T<sub>max</sub>:

$$4 \quad IR2T_{max} = -3.9759 * BasPoisChron + 15.769(r^2 = 0.61; p < 0.0001). \quad (1)$$

### 5 **3.1 IR2T<sub>max</sub> reconstruction**

6 IR2T<sub>max</sub> describes 410 years of maximum temperature of September with a cumulative  
7 monthly mean of 21-months meaning it has memory of the last two years. Temperature  
8 ranges from 13.52°C (-2.13°C with respect to the mean) in 1603 to 17.64°C n (+1.94°C with  
9 respect to the mean) in 2005 (Fig. 9). It is remarkable that the 12 years of the XXI century  
10 happen to be within the 25 warmest years. IR2T<sub>max</sub> covers a part of the Little Ice Age (Grove,  
11 1988) from 1602 to the end of the XIX century. The year-to-year temperature variability is  
12 3.92°C in the seventeenth century, 2.89°C in the eighteen century, 3.17°C in the nineteenth  
13 century and 3.07°C in the twentieth century. The seventeenth and eighteen centuries were the  
14 coldest of the reconstruction with 73% and 80% of the years with temperatures below the  
15 long-term mean, respectively. On the other hand, the nineteenth and the twentieth centuries  
16 were the warmest with 66% and 78% of the years exceeding the mean.

17 The main driver of the large-scale character of the warm and cold episodes may be changes in  
18 the solar activity (Fig.9). The beginning of the reconstruction starts with the end of the Spörer  
19 Minimum. The Maunder minimum, from 1645 to 1715 (Luterbach et al., 2001) seems to  
20 cohere with a cold period from 1645 to 1706. In addition, the Dalton minimum from 1796 to  
21 1830, is detected for the period 1810 to 1838. However, a considerably cold period from 1778  
22 to 1798 is not in consonance with a decrease in the solar activity. Four warm periods, 1626-  
23 1637, 1800-1809, 1845-1859 and 1986-2012, have been identified to cohere with increased  
24 solar activity. Overall, the correlation between the reconstruction and the solar activity is 0.34  
25 ( $p < 0.0001$ ), and increases to  $r = 0.49$  after 11-year low pass filtering the series, though the  
26 degrees of freedom are substantially reduced due to the increase autocorrelation.

27 The SEA (Fig.10) indicates some impact of volcanic eruptions on the short-term temperature  
28 variability within the reconstruction. It shows significance ( $p < 0.05$ ) decrease in September's  
29 temperature with a lag of three years.

1 Figure 11 shows the spatial correlation between the reconstruction and the CRU TS v.3.22 for  
2 Europe and northern Africa. High coefficient of determination ( $r^2 > 0.4$ ,  $p < 0.0001$ ) indicates a  
3 robust agreement and spatial extend of the reconstruction over the Iberian Peninsula (IP),  
4 especially for the central and Mediterranean Spain. The spatial correlation, however,  
5 decreases towards the southwest of the IP and the north of Europe.

6

#### 7 **4 Discussion and conclusion**

8 Based on a coherent network of 11 tree-ring sites in the IR including 316 TRW series we  
9 developed a 410-year maximum September temperature reconstruction. This record is the first  
10 climate reconstruction for the IR filling the gap between the temperature reconstructions  
11 developed for the north IP (Büntgen et al., 2008; Dorado-Liñán et al., 2012a, Esper et al.  
12 2015a) and for the southern IP (Dorado-Liñán et al, 2014). The IR2T<sub>max</sub> has been achieved  
13 using TRW as well as for the southern IP (Dorado-Liñán et al, 2014). However, for the  
14 Pyrenees, MXD (Büntgen et al., 2008, Dorado-Liñán et al., 2012a) or stable isotopes (Esper et  
15 al. 2015a) are needed to get skilful records for a temperature reconstruction.

16 The main statistics used to verify the accuracy of the reconstruction present similar values to  
17 those developed for the IP. For instance, the RE coefficient for the period 1945-2012 is 0.56  
18 meaning that the reconstruction has indeed useful skills to develop a reconstruction. A  
19 relatively high signal to noise ratio indicates there is meaningful climatic information in the  
20 chronology. The mean correlation between sites for the common period ( $r = 0.51$ , Fig. 3)  
21 reveals substantial agreement between the sites and species. Correlation is strongest among  
22 high elevation sites including the sites VIN and CAV which are both derived from *Pinus*  
23 *uncinata*. The mean chronology, with 35.40% of the first component variance and 48.52 of  
24 signal to noise ratio, captures the regional climate signal accurately, which highlights the  
25 beauty of regional averages (Briffa et al., 1998).

26 The original, raw chronology extended over the 1465-2012 period, some 150 years longer  
27 than the final reconstruction. However, due to low EPS values prior to 1602, which is related  
28 to the low number of samples the final reconstruction was developed for the period 1602-  
29 2012.

30 A novel detrending approach, considering a Basal Area-Poisson model instead of the  
31 traditional regional curve (Esper et al. 2003) has certainly improved the skill of the

1 reconstruction and enabled retaining high-to-low frequency climate variance. The traditional  
2 approach of using RCS with the mean TRW curve of the age-aligned data only reached  
3 correlations with the maximum temperature of September with a cumulative monthly mean of  
4 21 months up to  $r = -0.5$ , while with the new approach reached  $r = -0.78$ .

5 It is usually difficult to determine the extent to which the effects of environmental factors on  
6 tree growth depend on age (genetic control) and/or on size (physiological control), but recent  
7 investigations suggest that it is often the size, and not the age, that is important (Mencuccini et  
8 al. 2005; Peñuelas 2005). In fact, climate variability is more size-dependent than age or  
9 species (De Luis et al., 2009). Hence, the size-based standardization considered here  
10 maximizes the common signal. In addition, when combining TRW series from different sites  
11 and species, as done here, the heterogeneity in responses might be large. Therefore, size  
12 standardization may be a commendable solution to develop unbiased chronologies. Finally,  
13 the new method should be tested in other locations since it may help to maximizes responses  
14 especially in heterogeneous areas.

15 The development of climate parameters retaining temperature information of the past 3 years  
16 is certainly unusual and distinctive. However, memory effects in TRW data can arise from  
17 physiological processes already suggested by Schulman (1956) and Matalas (1962).  
18 Moreover, taking into account that TRW growth is conditioned by the storage of starch and  
19 sugar in parenchyma ray tissue, the remobilization of carbohydrates from root structures, and  
20 the development of needle enduring several growing seasons, influencing the radial increment  
21 beyond the instant impact of temperature variability (Pallardy, 2010), led us to add the  
22 cumulative monthly mean to the climate parameters. In fact, we demonstrated that the signal  
23 in the study area is magnified with a memory of 21 months from the previous September.  
24 Memory effects in TRW data have been also studied regarding the delayed response in TRW  
25 (1~5 years) to post volcanic eruptions associated with a decrease in current's year  
26 temperature (D'Arrigo et al., 2013, Esper et al., 2014). Thus, developing the two year  
27 memory IR2T<sub>max</sub> allowed us to maintain not only the low frequency signal, highlighting the  
28 warm and cold phases, which may be explained by the high correlation with solar activity  
29 during 410 years ( $0.34$ ,  $p < 0.001$ ), but also the high frequency signal, emphasizing the  
30 memory effects of the volcanic eruptions in TRW, already studied by Briffa et al. (1998) and  
31 recently by Esper et al. (2015b). According to the SEA (Fig.9), the volcanic eruptions have a  
32 significance reduction (95% confidence) of September's temperature ( $-1.98^{\circ}\text{C}$ ) with a three

1 years lag. However, the  $IR2T_{max}$  is already considering the two previous year's temperature,  
2 which means the temperature decrease occurred the year after the extreme volcanic event in  
3 consistency with (Frank et al., 2007a). The stability of the signal was assessed by a 30-y  
4 moving correlation from 1945 to 2012, which shows a better correlation for the period 1979-  
5 2012 in agreement with the raise of temperatures observed for last decades which may be  
6 limiting TRW growth and therefore magnifying the climate signal. However, the relationship  
7 between the chronology and the climate parameter chosen never drops from -0.54 within the  
8 calibration period 1945-2012. The negative correlation with maximum temperature of  
9 previous September is in concordance with the values detected in Cazorla by Dorado-Liñán et  
10 al. 2014. Presumably, a continuous rise in temperatures, as suggested by the IPCC (2013),  
11 will trigger an incessant decrease in the tree-ring growth.

12 Even though the CRU dataset extents the 1901-2013 period, the general distribution of  
13 meteorological observatories in Spain did not begin until the mid-twentieth century  
14 (Gonzalez-Hidalgo et al. 2011). In fact, the closest instrumental weather station, located in  
15 Vinuesa (Fig.1), began in 1945. However, due to the large amount of gaps in the time series,  
16 the CRU dataset was used instead for the split calibration/verification approach for the period  
17 1945-2012. The advantages of regional climatic averages were already addressed by Blasing  
18 et al. (1981) stating that the average climatic record of the gridded dataset over the study area  
19 is representative of the regional climatic conditions, and does not reflect microclimate  
20 conditions which may be characteristic of the climatic record at a single station. Tree-ring  
21 data might therefore have more variance in common with the regionally averaged climatic  
22 record than with the climatic record of the nearest weather station. Generally, studies have  
23 shown that the measurements of MXD produce chronologies with an improved climatic signal  
24 (Briffa et al., 2002) as it was revealed for summer temperature reconstructions (Hughes et al.,  
25 1984; Büntgen et al. 2008; Matskovsky and Helama, 2014). However, based on a TRW  
26 chronology, it is remarkable the high correlation coefficient for the full calibration period and  
27 the CRU dataset ( $r = -0.78$ ).

28 Throughout the  $IR2T_{max}$  reconstruction we identified the main warm and cold phases  
29 (Maunder minimum, Dalton minimum) related with long-term temperature variability  
30 generally attributed to changes in cycles of activity (Lean et al., 1995; Lassen et al. 1995;  
31 Haigh et al. 2015). In addition, similar cold and warm phases are observed comparing with  
32 the Pyrenees (Büntgen et al. 2008) and Cazorla (Dorado-Liñán et al. 2014) reconstructions.



1 However, previously to the Dalton minimum, a warm phase is detected in IR2T<sub>max</sub> and the  
2 Cazorla reconstruction although it is not present in the Pyrenees or in the Alps (Büntgen et al.,  
3 2011).

4 Through the spatial extent and magnitude of the IR2T<sub>max</sub> reconstruction over Europe it can be  
5 acknowledged that the reconstruction is effective and usable for most of the Spanish Iberian  
6 Peninsula. Working especially for the central and Mediterranean IP with very high coefficient  
7 of determination ( $r^2 > 0.4$ ).

8

## 9 **Acknowledgements**

10 This study was supported by the Spanish government (CGL2011-28255) and the government  
11 of Aragon throughout the Program of research groups (group Clima, Cambio Global y  
12 Sistemas Naturales, BOA 147 of 18-12-2002) and FEDER funds. Ernesto Tejedor is  
13 supported by the government of Aragon with a Ph.D. grant. Fieldwork was carried out in the  
14 province of Soria; we are most grateful to its authorities, for supporting the sampling  
15 campaign. We are thankful to Klemen Novak, Edurne Martinez, Luis Alberto Longares, and  
16 Roberto Serrano for help during fieldwork.

17

## 1 **5 References**

- 2 Akkemik, Ü., Da deviren., N., Aras, A.: A preliminary reconstruction (A.D. 1635–2000) of  
3 spring precipitation using oak tree rings in the western Black Sea region of Turkey. *Int J*  
4 *Biometeorol* 49(5):297–302, 2005.
- 5 Anchukaitis, K.J., Breitenmoser, P., Briffa, K.R., Buchwal, A., Büntgen, U., Cook, E.R.,  
6 D'Arrigo, R.D., Esper, J., Evans, M.N., Frank, D., Grudd, H., Gunnarson, B.E., Hughes,  
7 M.K., Kirilyanov, A.V., Körner, C., Krusic, P.J., Luckman, B., Melvin, T.M., Salzer, M.W.,  
8 Shashkin, A.V., Timmreck, C., Vaganov, E.A., Wilson, R.J.S.: Tree rings and volcanic  
9 cooling. *Nature Geoscience*, 5 (12), pp. 836-837, 2012.
- 10 Barriendos, M.: Climatic variations in the Iberian Peninsula during the late Maunder  
11 minimum (AD 1675-1715): An analysis of data from rogation ceremonies. *Holocene*, 7 (1),  
12 pp. 105-111, 1997.
- 13 Blasing, T. J., D. N. Duvick, and D. C. West: Dendroclimatic calibration and verification  
14 using regionally averaged and single station precipitation data, *Tree-Ring Bulletin*, 41, 37-43,  
15 1981.
- 16 Briffa, K.R. and Jones, P.D.: Basic chronology statistics and assessment. In: *Methods of*  
17 *Dendrochronology: Applications in the Environmental Sciences* (Eds. E.R. Cook and L.A.  
18 Kairiukstis), pp.137-152, 1990.
- 19 Briffa, K.R., Jones, P.D., Bartholin, T.S., Eckstein, D., Schweingruber, F.H., Karlén, W.,  
20 Zetterberg, P., Eronen, M.: Fennoscandian summers from ad 500: temperature changes on  
21 short and long timescales. *Climate Dynamics*, 7 (3), pp. 111-119, 1992.
- 22 Briffa, K.R., Jones, P.D., Schweingruber, F.H., Osborn, T.J.: Influence of volcanic eruptions  
23 on Northern Hemisphere summer temperature over the past 600 years. *Nature*, 393 (6684),  
24 pp. 450-455, 1998.
- 25 Briffa, K.R., Osborn, T.J., Schweingruber, F.H., Jones, P.D., Shiyatov, S.G., Vaganov, E.A.:  
26 Tree-ring width and density data around the Northern Hemisphere: Part 1, local and regional  
27 climate signals. *Holocene*, 12 (6), pp. 737-757, 2002.
- 28 Bunn, A.G.: A dendrochronology program library in R (dplR). *Dendrochronologia* 26:115–  
29 124, 2008.

30

- 1 Büntgen, U., Esper, J., Schmidhalter, M., Frank, D.C., Treydte, K., Neuwirth, B., Winiger,  
2 M.: Using recent and historical larch wood to build a 1300-year Valais-chronology. In:  
3 Gärtner H, Esper J, Schleser G (eds) TRACE 2: 85-92, 2004.
- 4 Büntgen, U., Esper, J., Frank, D.C., Nicolussi, K., Schmidhalter, M.: A 1052-year tree-ring  
5 proxy for Alpine summer temperatures. *Climate Dynamics*, 25 (2-3), pp. 141-153, 2005.
- 6 Büntgen, U., Frank, D., Grudd, H., Esper, J.: Long-term summer temperature variations in the  
7 Pyrenees. *Climate Dynamics*, 31 (6), pp. 615-631, 2008.
- 8 Camuffo, D., Bertolin, C., Barriendos, M., Dominguez-Castro, F., Cocheo, C., Enzi, S.,  
9 Sghedoni, M., della Valle, A., Garnier, E., Alcoforado, M.-J., Xoplaki, E., Luterbacher, J.,  
10 Diodato, N., Maugeri, M., Nunes, M.F., Rodriguez, R.: 500-Year temperature reconstruction  
11 in the Mediterranean Basin by means of documentary data and instrumental observations.  
12 *Climatic Change*, 101 (1), pp. 169-199, 2010.
- 13 Cook, E.R., Briffa, K., Shiyatov, S., Mazepa, V.: Tree-ring standardization and growth trend  
14 estimation. In: Cook ER, Kairiukstis LA (eds), *Methods of dendrochronology: applications in*  
15 *the environmental sciences*. Kluwer Academic Publishers, Dordrecht, pp 104–162, 1990.
- 16 Cook, E.R., Briffa, K.R., Jones, P.D.: Spatial regression methods in dendroclimatology: a  
17 review and comparison of two techniques. *International Journal of Climatology* 14, 379–402,  
18 1994.
- 19 Creus, J. and Puigdefabregas, J.: Climatología histórica y dendrocronología de *Pinus uncinata*  
20 *R*. *Cuadernos de Investigación Geográfica* 2(2): 17-30, 1976.
- 21 Creus, J., Puigdefabregas, J.: Climatología histórica y dendrocronología de *Pinus uncinata* *R*.  
22 *Cuad Investig Geográfica* 2(2):17–30, 1982.
- 23 Crowley, T.J.: Causes of climate change over the past 1000 years. *Science*, 289 (5477), pp.  
24 270-277, 2000.
- 25 Čufar, K., de Luis, M., Eckstein, D., Kajfez-Bogataj, L.: Reconstructing dry and wet summers  
26 in SE Slovenia from oak tree-ring series. *Int J Biometeorol* 52:607–615, 2008.
- 27 D'Arrigo, R., Wilson, R., Tudhope, A.: The impact of volcanic forcing on tropical  
28 temperatures during the past four centuries. *Nature Geoscience*, 2 (1), pp. 51-56, 2009.
- 29 D'Arrigo, R., Wilson, R., Anchukaitis, K. J.: Volcanic cooling signal in tree ring temperature  
30 records for the past millennium, *J. Geophys. Res. Atmos.*, 118, 2013.

- 1 de Luis, M., Novak, K., Čufar, K., Raventós, J.: Size mediated climate-growth relationships in  
2 *Pinus halepensis* and *Pinus pinea*. *Trees - Structure and Function*, 23 (5), pp. 1065-1073,  
3 2009.
- 4 Domínguez-Castro, F., García-Herrera, R., Ribera, P., Barriendos, M.: A shift in the spatial  
5 pattern of Iberian droughts during the 17th century. *Climate of the Past*, 6 (5), pp. 553-563,  
6 2010.
- 7 Dorado Liñán, I., Büntgen, U., González-Rouco, F., Zorita, E., Montávez, J.P., Gómez-  
8 Navarro, J.J., Brunet, M., Heinrich, I., Helle, G., Gutiérrez, E.: Estimating 750 years of  
9 temperature variations and uncertainties in the Pyrenees by tree-ring reconstructions and  
10 climate simulations. *Climate of the Past*, 8 (3), pp. 919-933, 2012.
- 11 Dorado Liñán, I., Zorita, E., González-Rouco, J.F., Heinrich, I., Campello, F., Muntán, E.,  
12 Andreu-Hayles, L., Gutiérrez, E.: Eight-hundred years of summer temperature variations in  
13 the southeast of the Iberian Peninsula reconstructed from tree rings. *Climate Dynamics*, 44 (1-  
14 2), pp. 75-93, 2014.
- 15 El Kenawy, A., López-Moreno, J.I., Vicente-Serrano, S.M.: Trend and variability of surface  
16 air temperature in northeastern Spain (1920-2006): Linkage to atmospheric circulation.  
17 *Atmospheric Research*, 106, pp. 159-180, 2012.
- 18 Esper, J., Cook, E.R., Krusic, P.J., Peters, K., Schweingruber, F.H.: Tests of the RCS method  
19 for preserving low-frequency variability in long tree-ring chronologies. *Tree-Ring Research*  
20 59, 81-98, 2003.
- 21 Esper, J., Büntgen, U., Luterbacher, J., Krusic, P.: Testing the hypothesis of post-volcanic  
22 missing rings in temperature sensitive dendrochronological data. *Dendrochronologia* 13, 216-  
23 222, 2013.
- 24 Esper, J., Schneider, L., Krusic, P.J., Luterbacher, J., Büntgen, U., Timonen, M., Sirocko, F.,  
25 Zorita, E.: European summer temperature response to annually dated volcanic eruptions over  
26 the past nine centuries. *Bulletin of Volcanology* 75, 2013.
- 27 Esper, J., Dũthorn, E., Krusic, P., Timonen, M., Büntgen, U.: Northern European summer  
28 temperature variations over the Common Era from integrated tree-ring density records. *J.*  
29 *Quat. Sci.* 29, 487–494, 2014.

- 1 Esper, J., Großjean, J., Camarero, J.J., García-Cervigón, A.I., Olano, J.M., González-Rouco,  
2 J.F., Domínguez-Castro, F., Büntgen, U.: Atlantic and Mediterranean synoptic drivers of  
3 central Spanish juniper growth. *Theoretical and Applied Climatology*, 2014.
- 4 Esper, J., Konter, O., Krusic, P., Saurer, M., Holzkämper, S., Büntgen, U.: Long-term summer  
5 temperature variations in the Pyrenees from detrended stable carbon isotopes.  
6 *Geochronometria* 42, 53-59, 2015.
- 7 Esper, J., Schneider, L., Smerdon, J.E., Schöne, B.R., Büntgen, U.: Signals and memory in  
8 tree-ring width and density data. *Dendrochronologia*, 35, pp. 62-72, 2015b.
- 9 Fischer, E.M., Luterbacher, J., Zorita, E., Tett, S.F.B., Casty, C., Wanner, H.: European  
10 climate response to tropical volcanic eruptions over the last half millennium, *Geophys. Res.*  
11 *Let.*, 34, L05707, 2007.
- 12 Frank, D., Esper, J., Cook, E.R.: On variance adjustments in tree-ring chronology  
13 development. In: Heinrich I et al. (Eds.) *Tree rings in archaeology, climatology and ecology*,  
14 *TRACE*, Vol. 4, 56-66, 2006.
- 15 Frank, D., Büntgen, U., Böhm, R., Maugeri, M., Esper, J.: Warmer early instrumental  
16 measurements versus colder reconstructed temperatures: shooting at a moving target.  
17 *Quaternary Science Reviews* 26, 3298-3310, 2007a.
- 18 Fritts, H.C., Guiot, J., Gordon, G.A., Schweingruber, F.H.: Methods of calibration,  
19 verification, and reconstruction. In *Methods of Dendrochronology*, 1990.
- 20 Fritts, H.C.: *Tree rings and climate*. Academic Press, London, 1976.
- 21 Giorgi, F., Lionello, P.: Climate change projections for the Mediterranean region, *Global and*  
22 *Planetary Change*, Volume 63, Issues 2–3, September, Pages 90-104, 2008.
- 23 González-Hidalgo, J.C., Brunetti, M., de Luis, M.: A new tool for monthly precipitation  
24 analysis in Spain: MOPREDAS database (monthly precipitation trends December 1945  
25 November 2005). *International Journal of Climatology*, 31 (5), pp. 715-731, 2011.
- 26 Gonzalez-Hidalgo, J.C., Peña-Angulo, D., Brunetti, M., Cortesi, N. MOTEDAS: A new  
27 monthly temperature database for mainland Spain and the trend in temperature (1951-2010).  
28 *International Journal of Climatology*, 2015.

1 Grudd, H.: Torneträsk tree-ring width and density ad 500-2004: A test of climatic sensitivity  
2 and a new 1500-year reconstruction of north Fennoscandian summers. *Climate Dynamics*, 31  
3 (7-8), pp. 843-857, 2008.

4 Guijarro, J.A.: Tendencias de la temperatura en España. En García Legaz, C. y Valero, C.  
5 (Coords). *Fenómenos meteorológicos adversos en España*. AEMET y CCS. Madrid, 2013.

6 Haigh, J.D., Cargill, P.: *The Sun's Influence on Climate*, pp. 1-207, 2015.

7 Harris, I., Jones, P.D., Osborn, T.J., Lister, D.H.: Updated high-resolution grids of monthly  
8 climatic observations - the CRU TS3.10 Dataset. *International Journal of Climatology*, 34 (3),  
9 pp. 623-642, 2014.

10 Hertig, E. and J. Jacobeit: Assessments of Mediterranean precipitation changes for the 21st  
11 century using statistical downscaling techniques. *International Journal of Climatology* 28(8):  
12 1025-1045, 2008.

13 Holmes, R.L.: Computer-assisted quality control in tree-ring dating and measurement. *Tree-*  
14 *Ring Bull* 43:69–78, 1983.

15 Hughes, M.K., Schweingruber, F.H., Cartwright, D., Kelly, P.M.: July-August temperature at  
16 Edinburgh between 1721 and 1975 from tree-ring density and width data. *Nature*, 308 (5957),  
17 pp. 341-344, 1984

18 IPCC, 2013: *Climate Change 2013: The Physical Science Basis*. Contribution of Working  
19 Group I to the Fifth Assessment Report of the Intergovernmental Panel on Climate Change  
20 [Stocker, T.F., D. Qin, G.-K. Plattner, M. Tignor, S.K. Allen, J. Boschung, A. Nauels, Y. Xia,  
21 V. Bex and P.M. Midgley (eds.)]. Cambridge University Press, Cambridge, United Kingdom  
22 and New York, NY, USA, 1535 pp, doi:10.1017/CBO9781107415324.

23 Larsson, L.A.: CoRecorder&CDendro program. Cybis Elektronik & Data AB. Version 7.6,  
24 2012.

25 Lassen, K., Friis-Christensen, E.: Variability of the solar cycle length during the past five  
26 centuries and the apparent association with terrestrial climate. *Journal of Atmospheric and*  
27 *Terrestrial Physics*, 57 (8), pp. 835-845, 1995.

28 Lean, J., Beer, J., Bradley, R.: Reconstruction of solar irradiance since 1610: implications for  
29 climate change. *Geophysical Research Letters*, 22 (23), pp. 3195-3198, 1995.

1 Lionello, P., Malanotte-Rizzoli, P., Boscolo, R., Alpert, P., Artale, V., Li, L., Luterbacher, J.,  
2 May, W., Trigo, R., Tsimplis, M., Ulbrich, U., Xoplaki, E.: The Mediterranean climate: An  
3 overview of the main characteristics and issues. *Developments in Earth and Environmental*  
4 *Sciences*, 4 (C), pp. 1-26, 2006a.

5 López-Moreno, J.I., El-Kenawy, A., Revuelto, J., Azorín-Molina, C., Morán-Tejeda, E.,  
6 Lorenzo-Lacruz, J., Zabalza, J., Vicente-Serrano, S.M.: Observed trends and future  
7 projections for winter warm events in the Ebro basin, northeast Iberian Peninsula.  
8 *International Journal of Climatology*, 34 (1), pp. 49-60, 2014.

9 Luterbacher, J., Rickli, R., Xoplaki, E., Tinguely, C., Beck, C., Pfister, C., Wanner, H.: The  
10 Late Maunder Minimum (1675-1715) - A key period for studying decadal scale climatic  
11 change in Europe. *Climatic Change*, 49 (4), pp. 441-462, 2001.

12 Luterbacher, J., Xoplaki, E., Casty, C., Wanner, H., Pauling, A., Küttel, M., Rutishauser, T.,  
13 Brönnimann, S., Fischer, E., Fleitmann, D., Gonzalez-Rouco, F.J., García-Herrera, R.,  
14 Barriendos, M., Rodrigo, F., Gonzalez-Hidalgo, J.C., Saz, M.A., Gimeno, L., Ribera, P.,  
15 Brunet, M., Paeth, H., Rimbu, N., Felis, T., Jacobeit, J., Dünkeloh, A., Zorita, E., Guiot, J.,  
16 Türkeş, M., Alcoforado, M.J., Trigo, R., Wheeler, D., Tett, S., Mann, M.E., Touchan, R.,  
17 Shindell, D.T., Silenzi, S., Montagna, P., Camuffo, D., Mariotti, A., Nanni, T., Brunetti, M.,  
18 Maugeri, M., Zerefos, C., Zolt, S.D., Lionello, P., Nunes, M.F., Rath, V., Beltrami, H.,  
19 Garnier, E., Ladurie, E.L.R.: Chapter 1 Mediterranean climate variability over the last  
20 centuries: A review, 2006.

21 Matalas, N.C.: Statistical properties of tree ring data. *Hydrol. Sci. J.* 7, 39–47, 1962.

22 Matskovsky, V.V., Helama, S.: Testing long-term summer temperature reconstruction based  
23 on maximum density chronologies obtained by reanalysis of tree-ring data sets from  
24 northernmost Sweden and Finland. *Clim.Past* 10, 1473–1487, 2014.

25 Mencuccini, M., Martínez-Vilalta, J., Vanderklein, D., Hamid, H.A., Korakaki, E., Lee, S.,  
26 Michiels, B.: Size-mediated ageing reduces vigour in trees. *Ecology Letters*, 8 (11), pp. 1183-  
27 1190, 2005.

28 Mitchell, V.L.: An investigation of certain aspects of tree growth rates in relation to climate in  
29 the central Canadian boreal forest. Technical report 33pp. Department of Meteorology,  
30 University of Wisconsin, 1967.

31 Pallardy, S.G.: *Physiology of Woody Plants*. Academic Press, 2010.

- 1 Panofsky, H.A., Brier, G.W.: Some applications of statistics to meteorology. University Park,  
2 Pennsylvania, p. 224, 1958.
- 3 Pena-Angulo, D., Cortesi, N., Brunetti, M., González-Hidalgo, J.C.: Spatial variability of  
4 maximum and minimum monthly temperature in Spain during 1981–2010 evaluated by  
5 correlation decay distance (CDD). *Theoretical and Applied Climatology*, 122 (1-2), pp. 35-45,  
6 2015.
- 7 Peñuelas, J.: Plant physiology—a big issue for trees. *Nature*, 437:965–966, 2005.
- 8 Rinn, F.: TSAPWin™ – Time series analysis and presentation for dendrochronology and  
9 related applications, Version 4.69, 2005.
- 10 Ruiz, P.: Análisis dendroclimático de *Pinus uncinata Ramond* en la Sierra Cebollera (Sistema  
11 Ibérico). *Cuadernos de Investigación Geográfica* 15(1-2): 75-80, 1989.
- 12 Ruiz-Flaño, P.: Dendroclimatic series of *Pinus uncinata* R. in the Central Pyrenees and in the  
13 Iberian System. A comparative study. *Pirineos* 132:49–64, 1988.
- 14 Sánchez, E., Gallardo, C., Gaertner, M.A., Arribas, A., Castro, M.: Future climate extreme  
15 events in the Mediterranean simulated by a regional climate model: A first approach. *Global  
16 and Planetary Change*, 44 (1-4), pp. 163-180, 2004.
- 17 Saz, M.A.: Análisis de la evolución del clima en la mitad septentrional de España desde el  
18 siglo XV a partir de series dendroclimáticas. Servicio de Publicaciones de la Universidad de  
19 Zaragoza, Zaragoza, 1105 pp, 2003.
- 20 Schulman, E.: *Dendroclimatic Changes in Semiarid America*. Tucson, University of Arizona  
21 Press, pp. 142, 1956.
- 22 Smith, J. G. and Weston, H. K.: Nothing particular in this year's history, *J. Oddball Res.*, 2,  
23 14-15, 1954.
- 24 Smith, J. G. and Weston, H. K.: Nothing particular in this year's history, *J. Oddball Res.*, 2,  
25 14-15, 1954.
- 26 Stokes, M.A., Smiley, T.L.: *An introduction to tree-ring dating*, 2<sup>nd</sup> edn. The University of  
27 Arizona Press, Tucson, 1968.



1 Tejedor, E., de Luis, M., Cuadrat, J.M., Esper, J., Saz, M.Á.: Tree-ring-based drought  
2 reconstruction in the Iberian Range (east of Spain) since 1694. *International Journal of*  
3 *Biometeorology*, 12 p, 2015.

4 Vicente-Serrano, S.M. and Cuadrat, J.M.: North Atlantic oscillation control of droughts in  
5 north-east Spain: Evaluation since 1600 A.D. *Climatic Change*, 85 (3-4), pp. 357-379, 2007.

6 Wigley, T.M.L., Briffa, K., Jones, P.D.: On the average value of correlated time series, with  
7 applications in dendroclimatology and hydrometeorology. *J Clim Appl Meteorol* 23:201–213,  
8 1984.

9

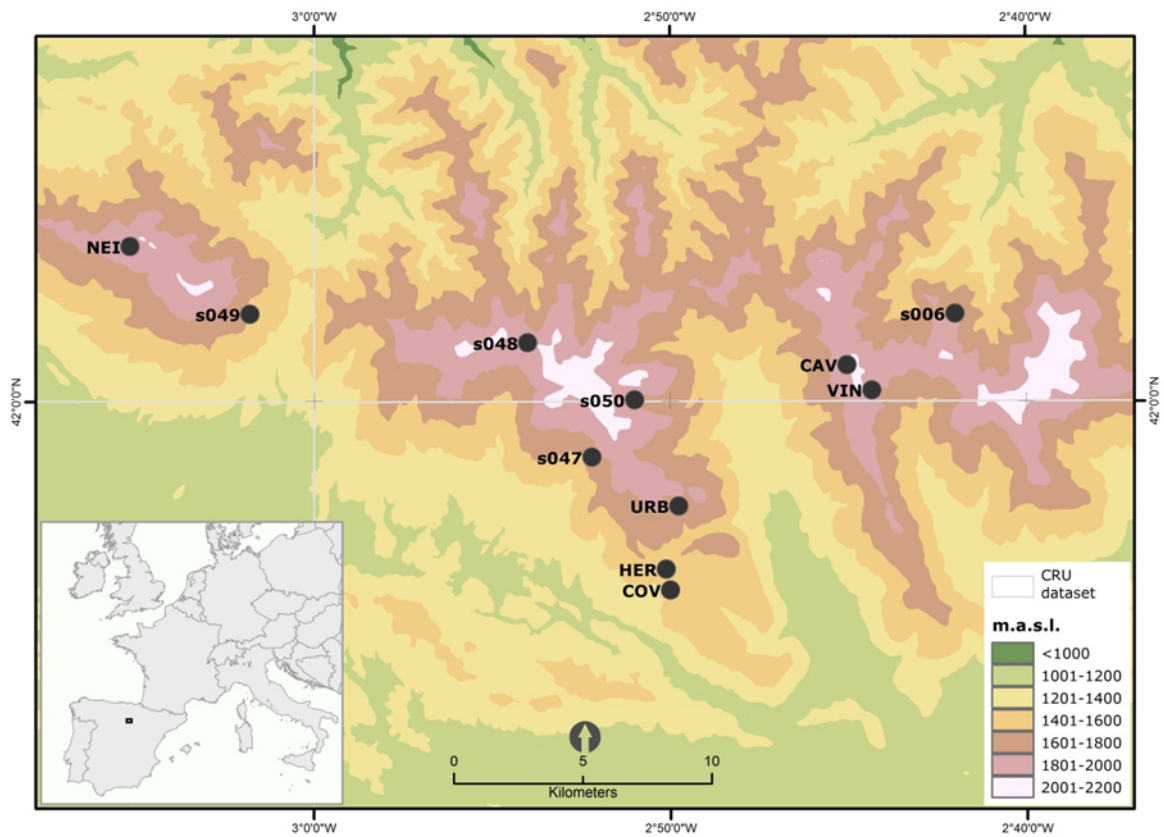
10

1 Table 1. Tree ring sites characteristics

Code	Site	Source	Lat	Long	Elevation	Species	Tree no	Sample no	Tree-rings	Period
s047	Urbión Covaleda	ITRDB	41.98	-2.87	1750	PISY	15	31	6549	1567- 1983
s048	Urbión Duruelo	ITRDB	42.02	-2.90	1840	PISY	8	17	3590	1671- 1983
s049	Urbión Quintenar	ITRDB	42.03	-3.03	1840	PISY	12	27	4713	1593- 1985
s050	Urbión Vinuesa	ITRDB	42.00	-2.85	1750	PISY	4	8	1942	1681- 1983
s006	Urbión	ITRDB	42.03	-2.7	1634	PISY	11	22	2397	1842- 1977
CAV	Castillo de Vinuesa	UNIZAR	42.01	-2.75	1900	PIUN	18	36	9236	1593- 2012
COV	Covaleda	IPE- CSIC- UNIZAR	41.93	-2.83	1500	PISY	16	48	14696	1568- 1993
HER	Barranco de las heridas	IPE- CSIC- UNIZAR	41.94	-2.84	1500	PISY	25	32	9347	1562- 1993
NEI	Neila	IPE- CSIC- UNIZAR	42.05	-3.08	1850	PISY	9	15	4822	1587- 1992

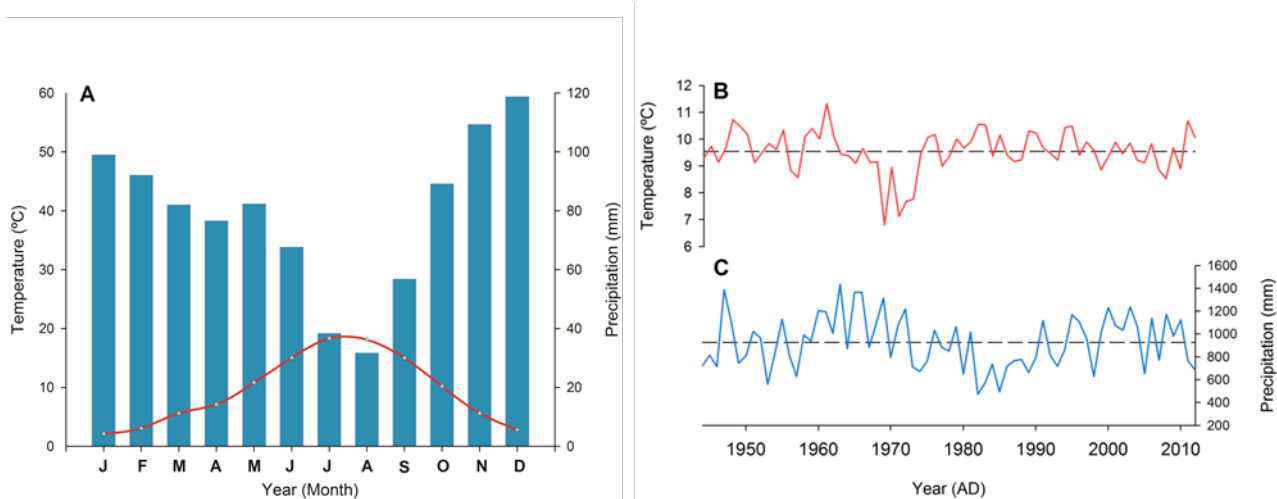
URB	Picos de Urbiión	UNIZAR	41.96	-2.82	1750	PISY	28	60	11328	1733-2012
VIN	Castillo de Vinuesa	IPE- CSIC- UNIZAR	42.03	-2.73	1900	PIUN	13	20	7653	1465-1992
Total							159	316	76273	

1 UNIZAR University of Zaragoza, IPE-CSIC Spanish National Research Council, ITRDB International Tree-Ring  
2 Databank

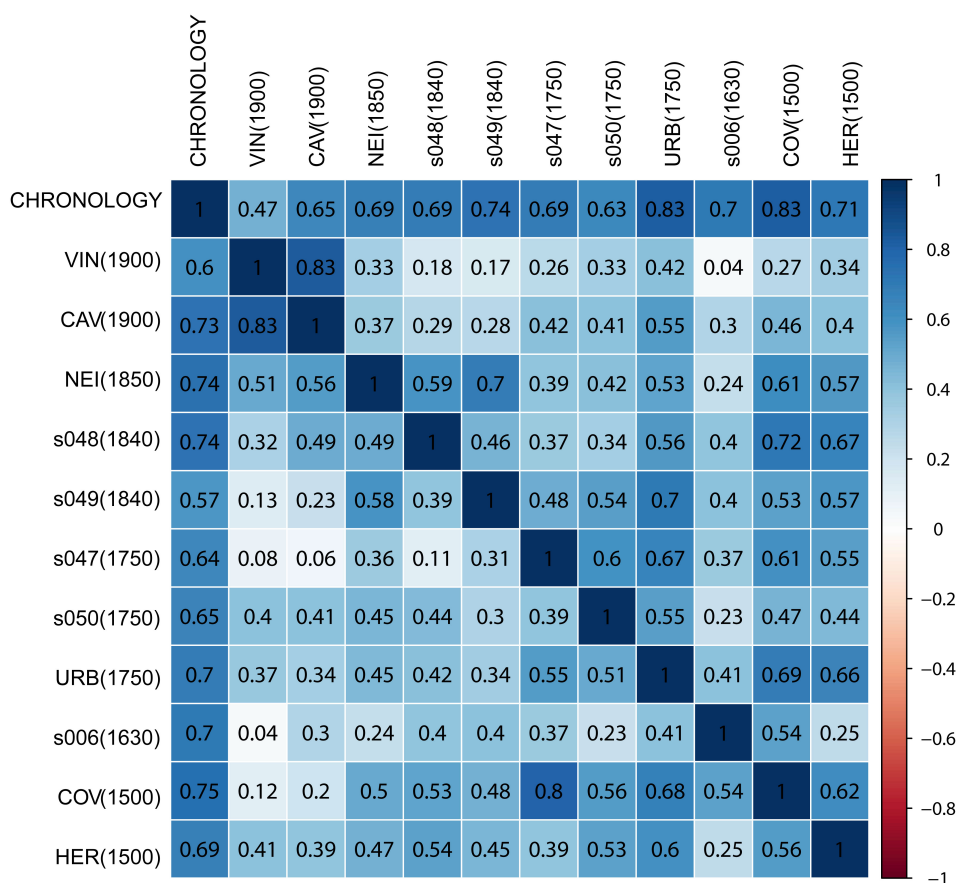


3  
4 Figure 1. Map showing the tree ring study sites and the climate data (CRU TS v.3.22) grid  
5 points in the Western Iberian Range (Soria).

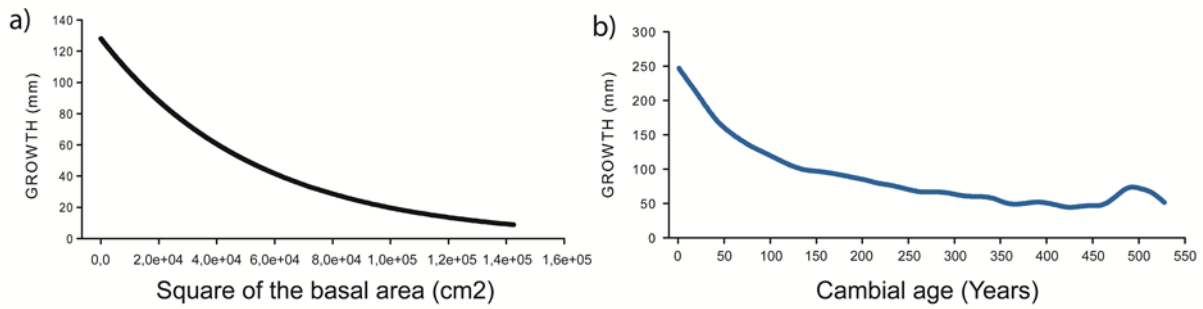
6  
7  
8  
9



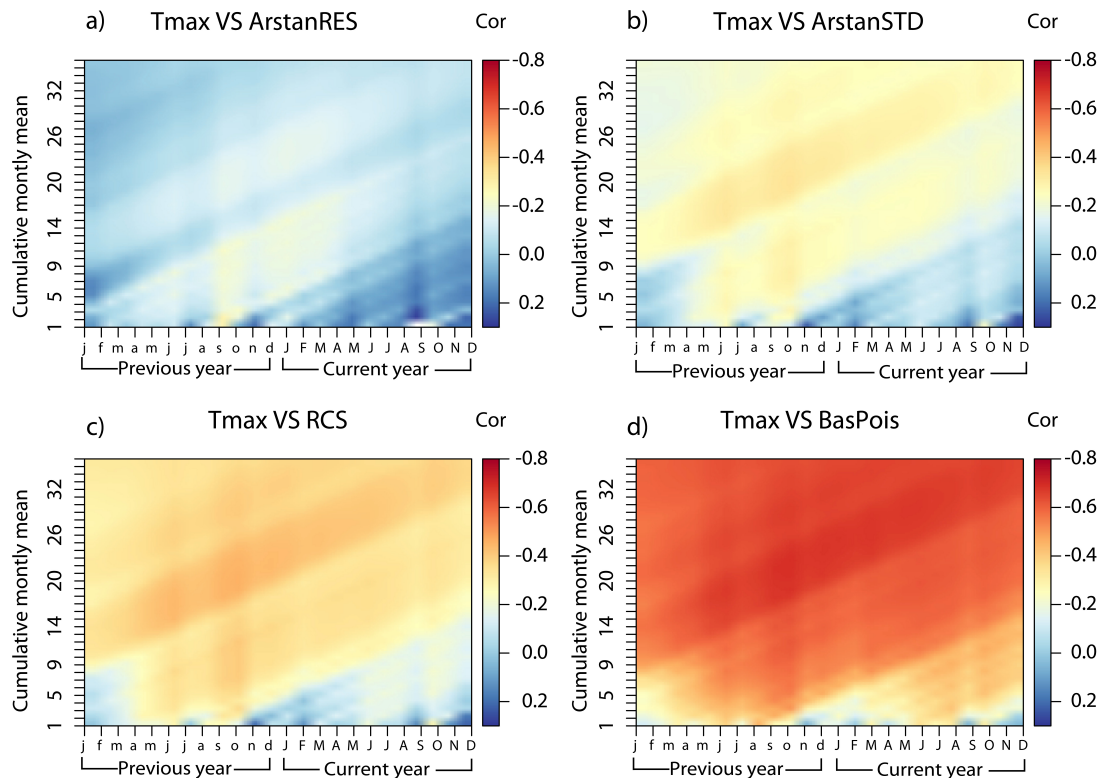
1  
 2 Figure 2. Climate diagram (A), mean temperature (B), mean precipitation (C) calculated using  
 3 data from CRU TS v.3.22 over the period 1944-2012 (Harris et al 2014).



4  
 5 Figure 3. Inter correlation of the raw chronologies between sites and the regional chronology,  
 6 sorted by elevation. Top right shows the correlations calculated over the common period  
 7 1842-1977. Bottom left shows the correlation over the full period of overlap between pairs of  
 8 chronologies

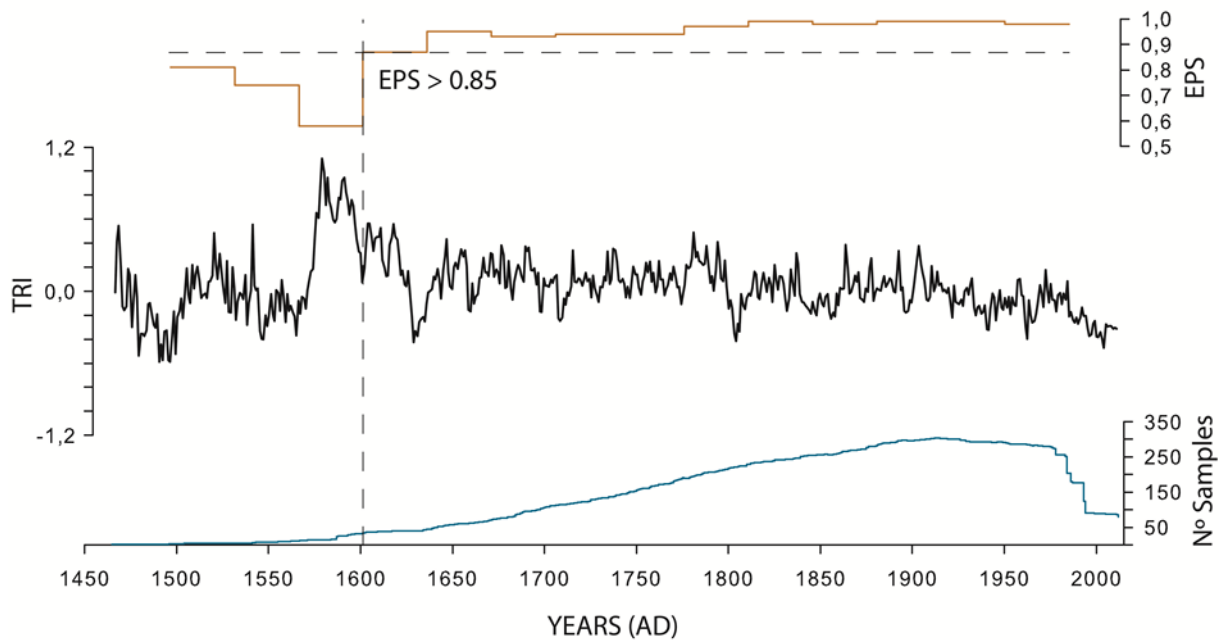


1  
 2 Figure 4. a) Represents the model of the BasPois method, b) represents the regional curve of  
 3 the RCS method.

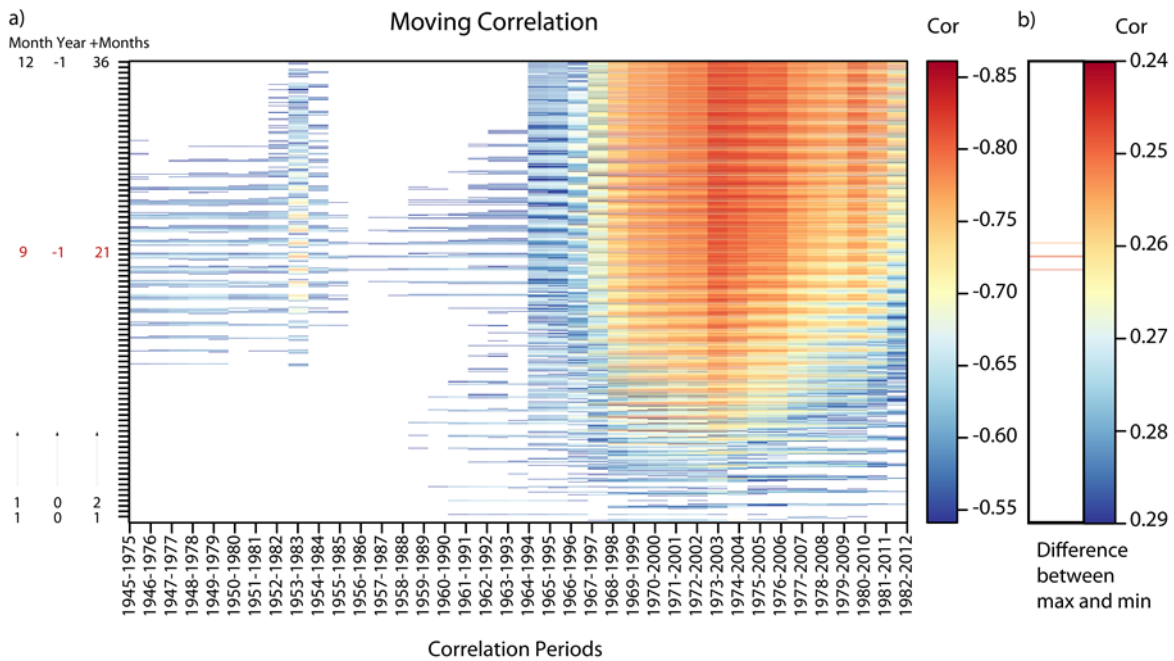


4  
 5 Figure 5. Correlation between the maximum temperature (from January of the previous year  
 6 to December of the current year with a cumulative monthly mean from 1 to 36 months) and  
 7 the residual Arstan chronology (a), the standard Arstan chronology (b), the RCS standard  
 8 chronology (c) and the Basal Area-Poisson standard chronology (d).

9

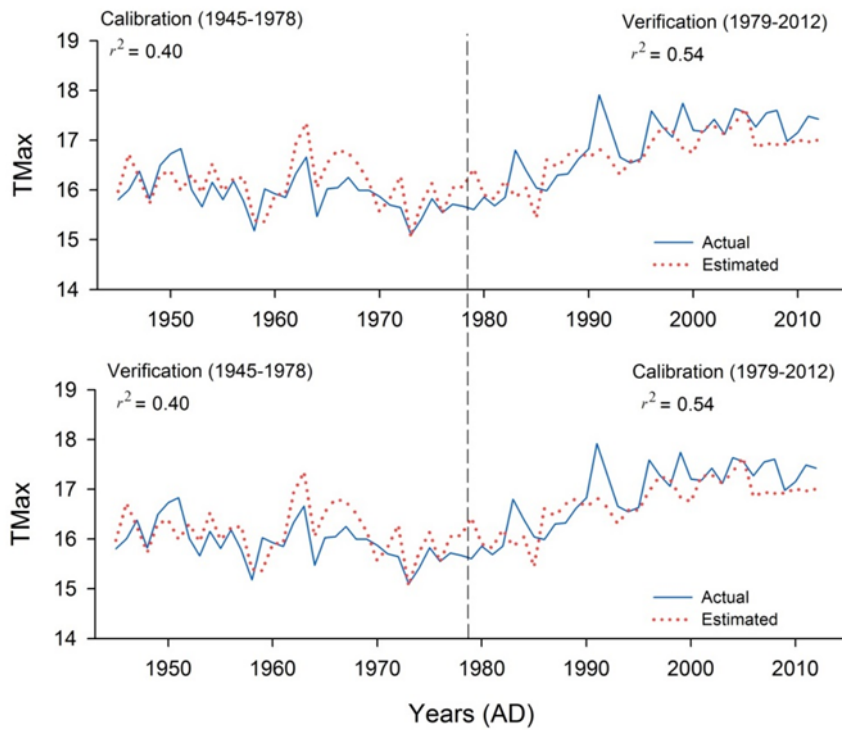


1  
 2 Figure 6. BasPois chronology (in black), number of samples (blue) and EPS statistic  
 3 (computed over 30-y window lagged by 15 years) back to 1465. Vertical dashed line  
 4 highlights the EPS=0.85 threshold in 1602.

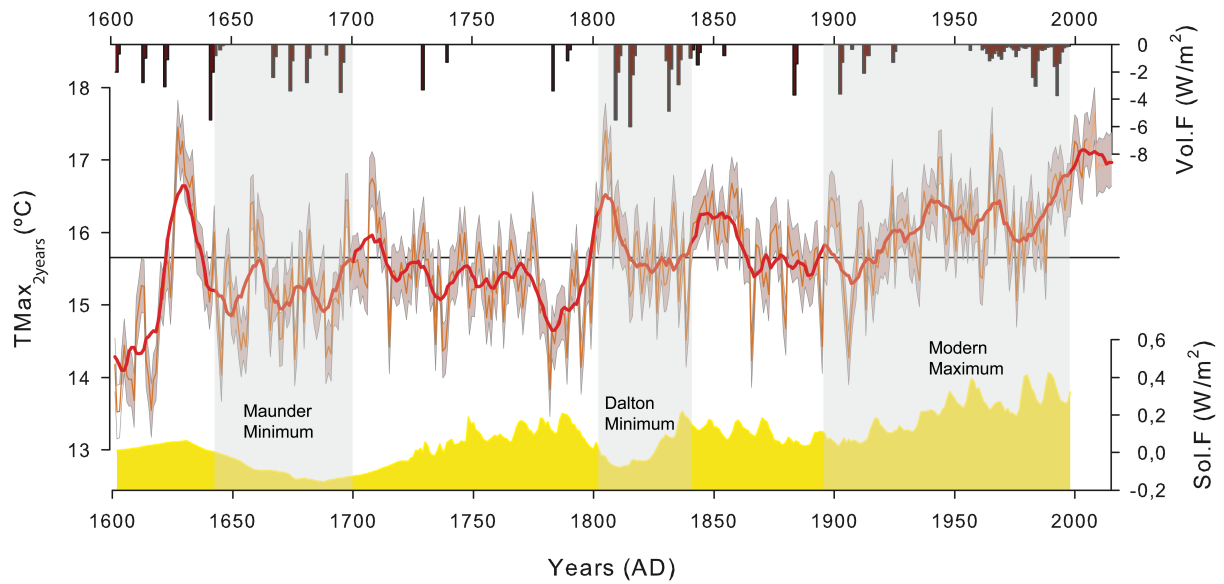


5  
 6 Figure 7.a) 30-year moving correlation from 1945 to 2012 between the maximum  
 7 temperature, from January of the current year (1,0,1) to December of the previous year (12, -  
 8 1, 36) with a cumulative monthly mean from 1 to 36 months and the BasPois chronology. Red  
 9 numbers indicates the chosen climatological parameter; 9, September, -1, previous year, 21,

1 months used for the cumulative monthly mean. b) The four best parameters are represented.  
2 Reddish line indicates the least difference between the maximum and minimum correlation in  
3 the correlation periods.



20 Figure 8. Calibration and verification results of the CRU data based  $T_{max_{Sep-1}}$  reconstruction



1 Figure 9. IR2T<sub>max</sub> reconstruction since AD 1602 for the Iberian Range. Bold red curve is a 11-  
 2 year running mean, purple shading indicates the mean square error based on the calibration  
 3 period correlation. Yellow shading at the bottom show solar forcing and bars on top indicate  
 4 volcanic forcings (Crowley 2000).

5

	Calibration 1945-1978	Verification 1978-2012	Calibration 1979-2012	Verification 1945-1978	Period 1945-2012
Years	34	34	34	34	68
Correlation	-0.64	0.73	-0.74	0.64	-0.78
R <sup>2</sup>	0.41	0.55	0.55	0.41	0.61
MSE	0.43	0.42	0.42	0.43	0.86
Reduction of error	0.40	0.65	0.65	0.40	0.56
Sing test	28+/6-	24+/10-	28+/6-	24+/10-	52+/16-

6 Table 2. Calibration/verification statistics of the T<sub>max</sub><sub>Sep-1</sub> reconstruction

7

8

9

10



1  
2  
3  
4  
5  
6  
7  
8  
9

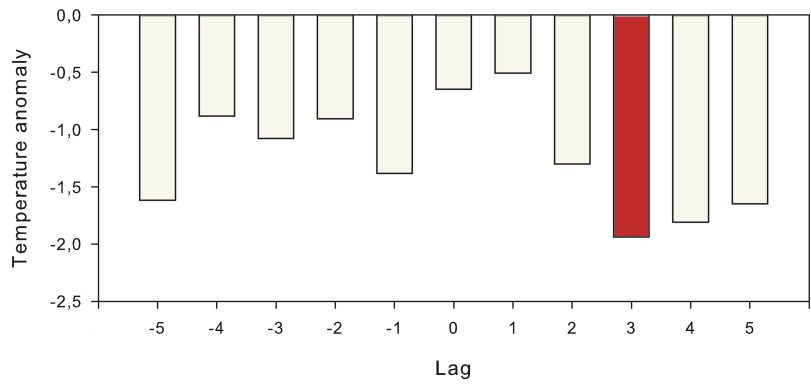


Figure 10. Superposed epoch analysis with a back and forward lag of 5 years. Significance ( $p < 0.05$ ) at 3 years after the extreme volcanic event.

10  
11  
12  
13  
14

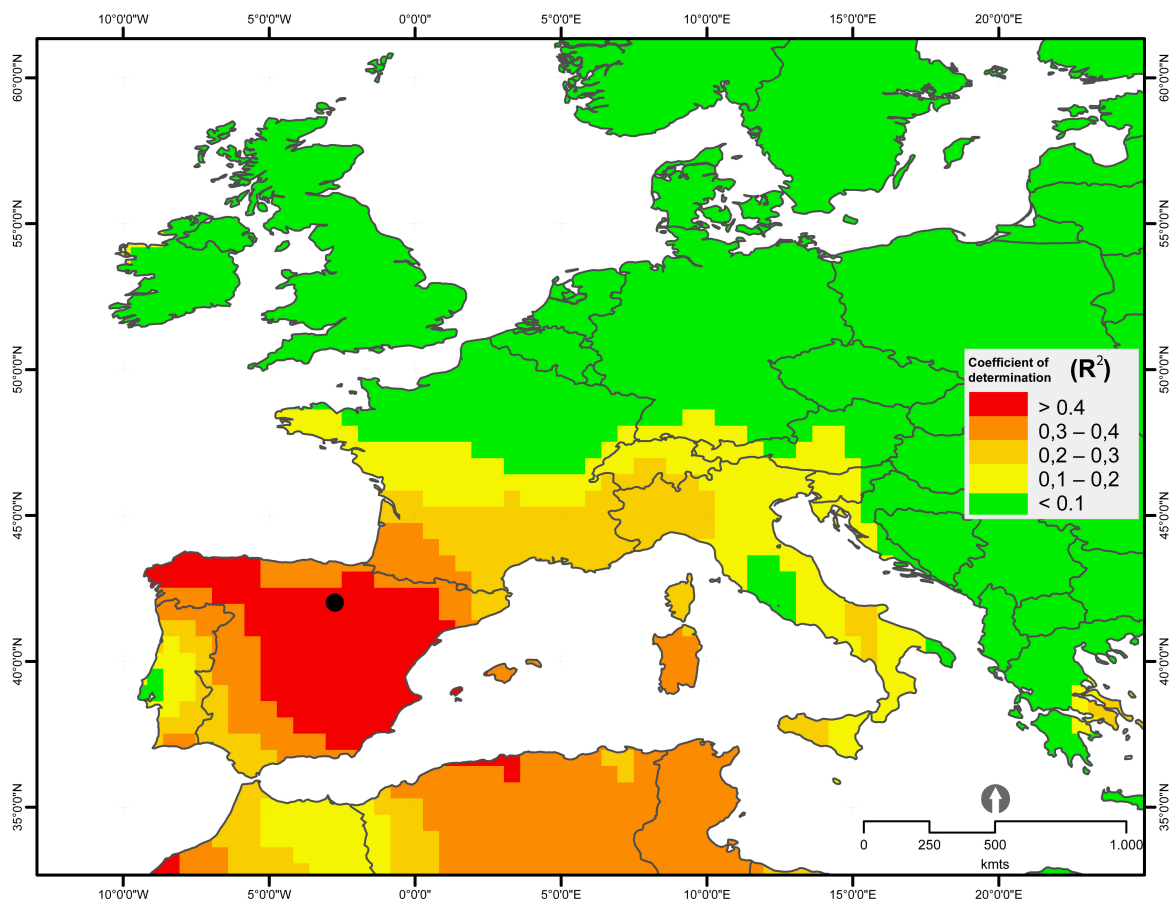


Figure 11. Map showing the spatial correlation patterns of the BasPois chronology with the gridded September of the previous year with a cumulative monthly mean of 21 months data. Correlation values are significant at  $p < 0.0001$ .